1

Introduction and Characteristics

Yong-Bin Wang, Shao-Hua Xiang, and Bin Tan

Department of Chemistry, Southern University of Science and Technology, No. 1088, Xueyuan Rd., Nanshan District, Shenzhen, 518055, China

1.1 Introduction and Classification

If a rigid object or the spatial arrangement of points including atoms is nonsuperposable on its mirror image, such an object possesses no symmetry elements of the second kind and the geometric property displayed is denoted as chirality (IUPAC). Chirality is widely represented in nature and plays crucial roles in life-sustaining processes. In living systems, chiral homogeneity of monomer units (such as α-amino acid and nucleoside) is found to induce more rapid polymerization and longer chain length of biopolymers (proteins, DNA, or RNA). Thus, the biomacromolecules assembled from the homochiral monomeric building blocks exhibit homochirality, which is considered the sine qua non for molecule-based life. As such, virtually all chiral biomolecules including small monomers and biopolymers in living organisms are enantiomerically pure to engender biological homochirality. This affects the differential interactions between biomacromolecules with a pair of enantiomers [1]. For this reason, pharmaceuticals development is progressively gravitating toward deriving single isomers instead of racemates [2, 3]. In the domain of material science, chiral homogeneity is critical for the properties of materials [4, 5]. Taken together, asymmetric synthesis toward molecular targets with high stereochemical purities has been a central research theme in many organic chemistry-oriented research laboratories.

Early investigations of asymmetric chemistry have centered on central chirality, which refers to stereoisomerism that arises from asymmetric spatial arrangement of a set of ligands attached to an atom (C_{abcd}, N_{abcd}^{+}, and $P(X)_{abc}$). With the progression of chemical science, additional types of stereoisomerisms began to garner increasing attention. Stereoisomers that feature axial chirality, helical chirality, and planar chirality assume different topological structures, but unlike those projecting central chirality, they exist as enantiomers in the absence of stereogenic center. Axial chirality refers to stereoisomerism resulting from nonplanar arrangement of four groups in pairs about a chirality axis (IUPAC). In diverse conformational topologies, atropisomers [6], chiral allenes [7], spiranes [8], and spiro chiral molecules [9] fulfill the definition of axial chirality. Among these

Axially Chiral Compounds: Asymmetric Synthesis and Applications, First Edition. Edited by Bin Tan.

axially chiral structures, atropisomers are unique in that the chirality is derived from restricted rotation about a single bond (chiral axis) and racemization proceeds simply through the rotation of this axis rather than the breaking and forming of chemical bond [6, 10] (Figure 1.1).

Central Chirality: Stereoisomerism resulting from the asymmetric spatial arrangement of a set of ligands attached to an atom (C_{abcd}, N_{abcd}^{+}, and $P(X)_{abc}$).
Helical Chirality: Stereoisomerism resulting from the arrangement of atoms in molecules along screw rotation.
Planar Chirality: Stereoisomerism resulting from the arrangement of out-of-plane groups with respect to a plane (chirality plane)
Axial Chirality: Stereoisomerism resulting from the nonplanar arrangement of four groups in pairs about a chirality axis.
Atropisomerism: Subclass of axial chirality; stereoisomerism resulting from the restricted rotation about a single bond.

When Christie and Kenner made the seminal discovery of atropisomerism in 1922, the importance of axial chirality has been largely overlooked until 1980. Noyori and coworkers developed and illustrated the superiority of axially chiral 1,1-biphenyl-derived 2,2′-bis(diphenylphosphino)-1,1′-binaphthyl (BINAP) as a chiral ligand for asymmetric metal-catalyzed reaction [11]. This work spurred the development of several excellent ligands derived from axially chiral 1,1-biphenyl and related spiro frameworks [9]. 1,1′-Bi-2-naphthol (BINOL), as one representative axially chiral reagent, finds utility as a ligand in metal catalysis and also asymmetric organocatalysis [12]. The formative works of Akiyama and Terada revealed the valuable potential of axially chiral BINOL-derived phosphoric acids as robust hydrogen-bonding catalysts in asymmetric Mannich reactions [13, 14]. Their discovery spawned intense research into organocatalysis and chiral Brønsted acid catalysis, from where the application of axially chiral skeletons in asymmetric catalysis vastly expanded. It is especially noteworthy that existing axially chiral catalysts, by empowering new stereoselective reaction manifolds, could in turn expedite the discovery of novel and more efficient axially chiral ligands/organocatalysts. Given many factors often govern the activity and stereoselectivity of catalysts/ligands, axially chiral architectures present high structural adaptability to

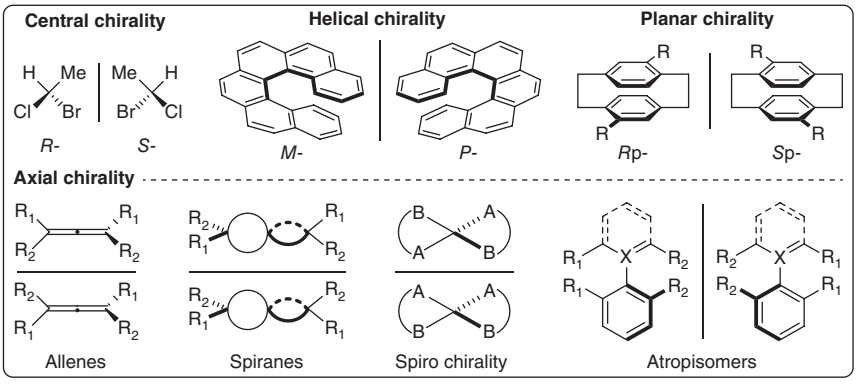

Figure 1.1 Various forms of chiralities and axial chiralities.

meet requirements of different catalytic reactions through convenient adjustment of their dihedral angles and substituents. To date, diverse types of axially chiral ligands and organocatalysts with highly enabling performance have been developed and constitute the most extensively used class of ligands in asymmetric catalysis [10, 15, 16] (Figure 1.2).

In addition to atropostable analogs, conformationally more labile tropos ligands, characterized by high interconversion rate between enantiomers that could preclude isolation of single enantiomers, can be evolved toward integration in asymmetric catalysis. Herein, chiral activator preferentially induces redistribution of the atropisomeric composition of these ligands to single atropisomer through coordination to transition metal, even with the use of catalytic amount per tropos ligands [17]. This section will be discussed in Chapter 11 (Figure 1.3).

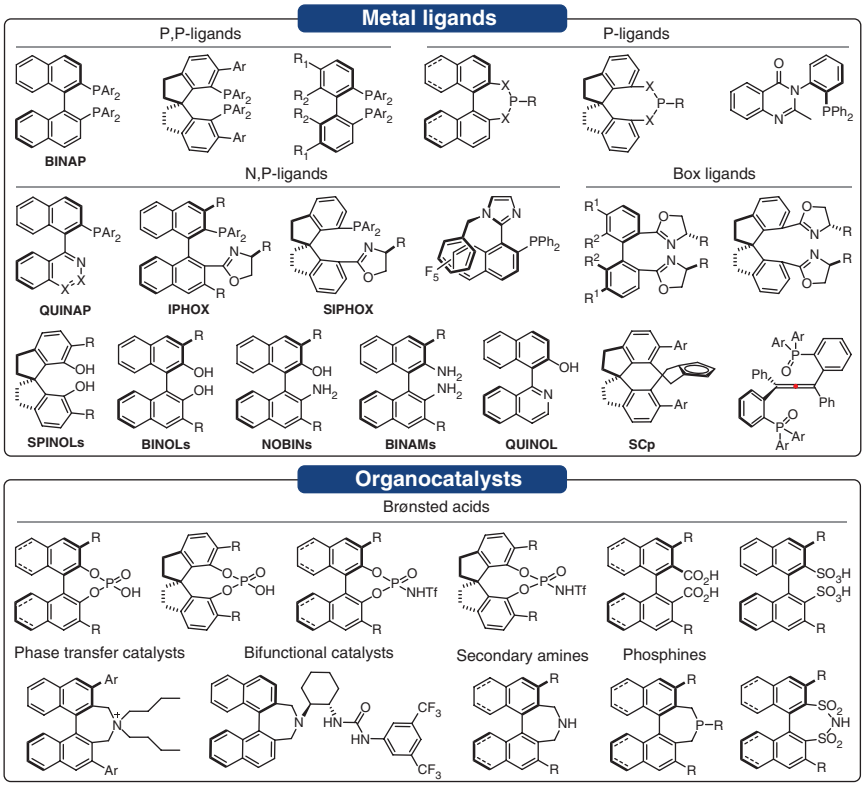

Figure 1.2 Representative organocatalysts and ligands containing axial chirality.

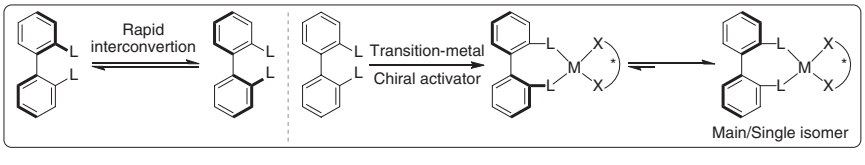

Figure 1.3 Tropos ligands.

Chiral biaryl or heterobiaryl axis is innate in many naturally occurring compounds where axial chirality could and often present in conjunction with other stereogenic elements. Therefore, natural products possessing axial stereogenicity could exhibit high structural diversity, from structurally sophisticated heptapeptide *vancomycin* to simple biaryls. The iconic antibiotic, *vancomycin*, contains numerous stereocenters, two chiral planes, and a rotationally hindered biaryl axis. The configurationally locked axis rigidifies the three-dimensional framework thus enhances its efficient binding with the bacterial target, resulting in remarkable bioactivities. Naturally occurring atropisomers are generally isolated in enantiopure or racemic form [18]. Although modern bioassays have revealed the huge biological activity differences elicited by two atropochiral antipodes, several marketed drugs bearing stable chiral axes are used in racemic form. Efforts dedicated in interrogating activity differences between enantiomeric atropisomers through structure–activity relationship (SAR) studies have resulted in highly active and selective axially chiral candidates [19, 20]. The promising biological activities of enantiopure atropisomers render research into biological enantioselectivity of axially chiral compounds high desirable (Figure 1.4).

Determining absolute configuration and enantiomeric purity of chiral compounds is one important if not mandatory procedure in the preparations of chiral compounds as well as in the research of biological enantioselectivity. Axially chiral skeletons have served well in this capacity, where they have been successfully applied in several characterization techniques based on chiral recognition. For example, the BINOL-derived chiral stationary phases for high-performance liquid chromatography (HPLC) aptly resolve a wide range of racemates containing amino group in diverse mobile-phase modes [21]. The fluorescent probe equipped with atropisomeric biphenyl skeleton can determine the enantiomeric excess (ee) of chiral hydroxycarboxylic acids and N-protected amino acids through fluorescent enhancement. The exquisite chiral recognition ability also enables real-time ee detection of asymmetric catalytic reaction, an application that is highly serviceable in optimization studies and one that is hardly achieved with conventional chiral HPLC [22, 23]. On top of chiral recognition, atropisomers are employed as chiral dopants of cholesteric liquid crystals since 40 years ago, a utility fostered by their ultrawide helical twisting power (up to $757\,\mu m^{-1}$) [24]. Amalgamation of this property with cholesteric liquid crystals provide valuable stimulus-responsive optical device [25] (Figure 1.5).

In summary, axial chirality is ubiquitously encountered and increasingly exploited in organic synthesis, asymmetric catalysis, research of medicinal chemistry, and functional materials [10, 18, 26–28]. This supplies steady demand to stimulate development of novel axially chiral scaffolds as well as preparations of the privileged ones in higher efficiency. Chiral resolution of racemates represents one stalwart method to obtain enantiopure axially chiral compounds. Before Tan's report on enantioselective catalysis method in 2016 [29], enantiomerically enriched SPINOL skeletons have been routinely procured via chiral resolution with L-menthol [30] or cinchona alkaloid derivative [31], implying the necessity to use excess chiral materials. The chiral auxiliary-assisted reaction [18, 32] and stereoselective oxidative homo-coupling [33] are two earliest successful attempts in straightforward construction of atropisomeric biaryls. Although stoichiometric or even superstoichiometric chiral reagents are still required, these reactions are forerunner to catalytic synthesis of enantiopure axially chiral skeletons. The catalytic construction of axially chiral skeletons [27] such as atropochiral biaryls and allenes [7] has been foremostly realized within the

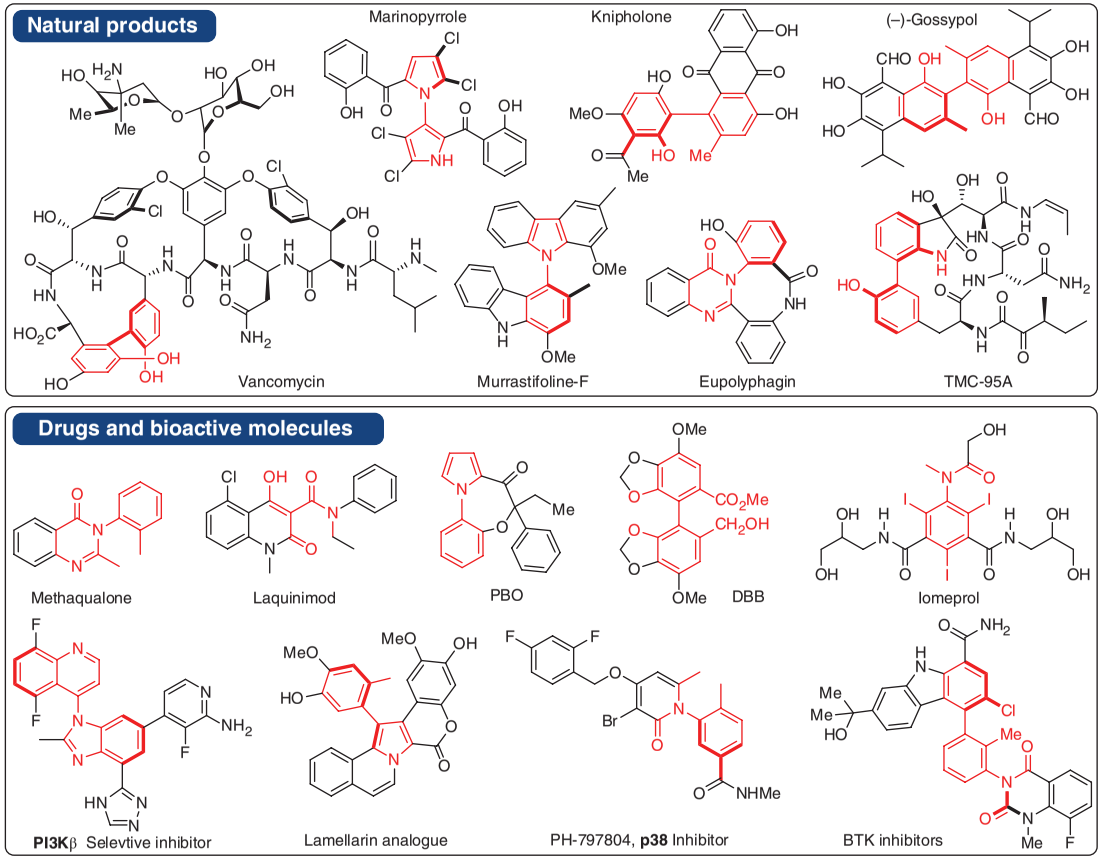

Figure 1.4 Natural products and bioactive molecules containing axial chirality element.

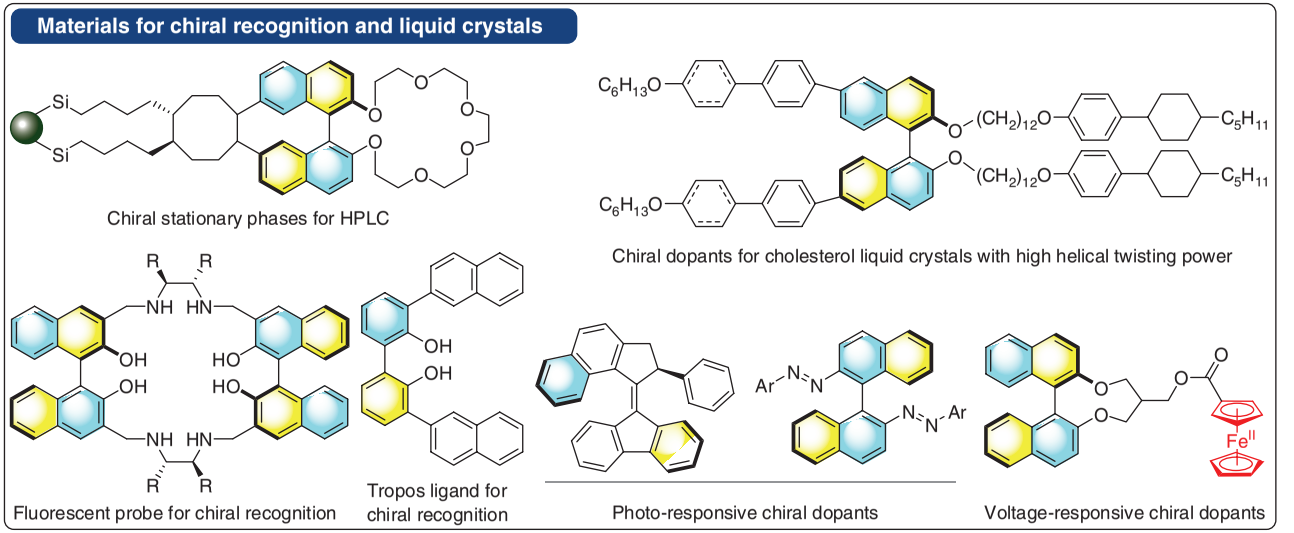

Figure 1.5 Axially chiral materials for chiral recognition and liquid crystals.

realm of asymmetric metal catalysis. This strategy has since undergirded the development of abundant and more efficient methodologies. Organocatalysis stepped into the limelight at the turn of the millennium and has evolved to turn into indispensable tool in contemporary asymmetric synthesis with its wide-ranging catalytic modes comprising hydrogen-bonding catalysis, Lewis base catalysis, and covalent catalysis. Atropisomer-selective synthesis has largely benefited from this advancement of organocatalysis; revelation of new atropisomeric scaffolds that could supplement the existing core members has been promoted [10]. This has opened up new chemical space for medicinal chemistry and materials.

1.2 Specification of Configuration

The R/S stereodescriptors are usually assigned to chiral compounds with reference to Cahn–Ingold–Prelog priority rules [34–39]. For the specific context of axial chirality, guidelines delineated below could be followed, which can be employed for allenes, spiranes, and analogs [40, 41]:

(1) Target chiral molecule is arbitrarily viewed from one side along the chiral axis; (2) Fischer projection of the molecule is formed by setting the two groups nearer to eyes as horizontal axis; (3) in accord with Cahn–Ingold–Prelog priority rules, the priority of this pair on the horizontal axis is evaluated and ranked as highest priority (1) and second highest priority (2); (4) the group with higher priority on the vertical axis is set as third in order (3); and (5) the R/S configuration of the molecule is determined according to the direction of the line connecting the three groups in order from 1 to 3. A clockwise path represents *R* configuration and an anticlockwise path represents *S* configuration (Figure 1.6).

With a modification of second step, this assignment process is relevant for atropisomeric biaryls, heterobiaryls, as well as anilines. In this case, the Fischer projection of the target chiral molecule is instead formed using the two pairs of groups flanking the rotation axis and the pair nearer to the eyes is taken as the horizontal axis (Figure 1.7).

In compounds exemplified above, each Fischer projection features only four bonds. The Fischer projections of some atropisomers, such as chiral alkenes, could however depict five bonds where there will be one set of two bonds along one of the four directions. When assigning the priority of the substituents according to Cahn–Ingold–Prelog priority rules,

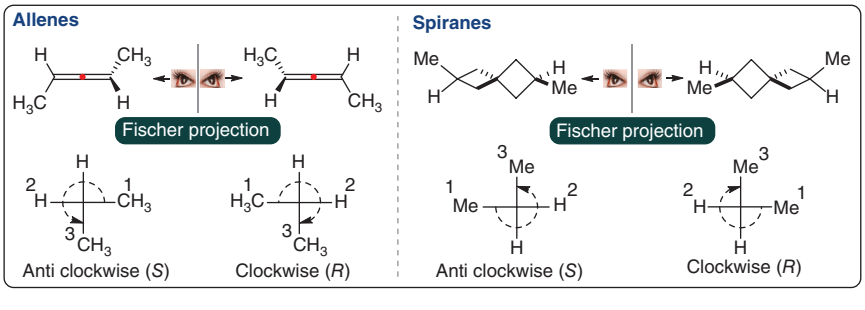

Figure 1.6 Chirality determination of axially chiral allenes and spiranes.

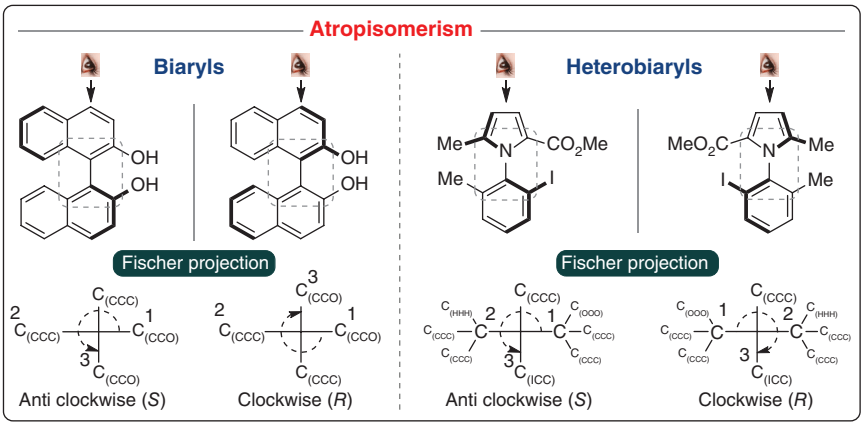

Figure 1.7 Chirality determination of atropisomeric (hetero)biaryls.

the substituents on the set of two bonds will be considered as one CC unit, which has a priority ranked between N and C (N > CC > C) (Figure 1.8).

As axially chiral molecules, stereogenic axis in spiro chiral compounds, on the other hand, may not immediately obvious. According to Cahn–Ingold–Prelog priority rules [36], the following sequence of steps is formulated to determine the *R/S* configuration:

(1) The axially chiral molecule is viewed from one spiro cycle to the other spiro cycle; (2) Fischer projection of the chiral molecule is formed using the pair of groups attached to spiro atom nearer to eyes as the horizontal axis; (3) based on Cahn–Ingold–Prelog priority rules, the group with higher priority on horizontal axis and vertical axis are respectively assigned as highest priority (1) and second highest priority (2); (4) the lower priority group on the horizontal axis is then assigned as third in order (3) (assignments in steps 3 and 4 in this scenario differ from that applied to chiral allenes and spiranes); and (5) the *R/S* configuration of the molecule is assigned according to the direction of the line connecting the

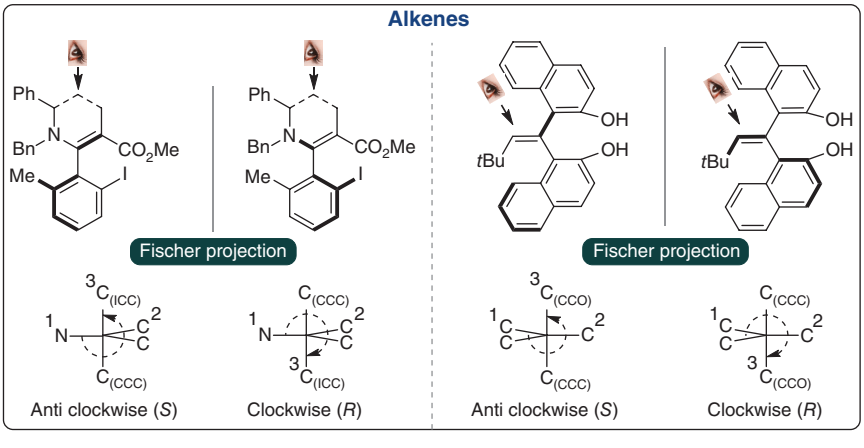

Figure 1.8 Chirality determination of axially chiral alkenes.

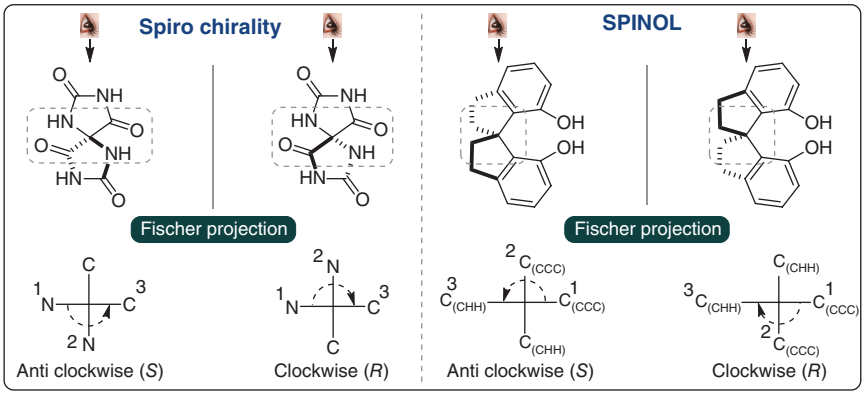

Figure 1.9 Chirality determination of Spiro skeletons.

three members in order from 1 to 3. A clockwise path represents *R* configuration and the anticlockwise path represents *S* configuration (Figure 1.9).

References

1 Barron, L.D. (2008). *Space Sci. Rev.* 135: 187–201.
2 Eriksson, T., Björkman, S., Roth, B. et al. (1995). *Chirality* 7: 44–52.
3 Shah, R.R., Midgley, J.M., and Branch, S.K. (1998). *Adverse Drug React. Toxicol. Rev.* 17: 145–190.
4 Shen, J. and Okamoto, Y. (2016). *Chem. Rev.* 116: 1094–1138.
5 Dyer, D.J., Schröder, U.P., Chan, K.P., and Twieg, R.J. (1997). *Chem. Mater.* 9: 1665–1669.
6 Kumarasamy, E., Raghunathan, R., Sibi, M.P., and Sivaguru, J. (2015). *Chem. Rev.* 115: 11239–11300.
7 Huang, X. and Ma, S. (2019). *Acc. Chem. Res.* 52: 1301–1312.
8 Krow, G. and Hill, R.K. (1968). *Chem. Commun.*: 430–431.
9 Xie, J.-H. and Zhou, Q.-L. (2008). *Acc. Chem. Res.* 41: 581–593.
10 Wang, Y.-B. and Tan, B. (2018). *Acc. Chem. Res.* 51: 534–547.
11 Miyashita, A., Yasuda, A., Takaya, H. et al. (1980). *J. Am. Chem. Soc.* 102: 7932–7934.
12 Brunel, J.M. (2007). *Chem. Rev.* 107: PR1–PR45.
13 Akiyama, T., Itoh, J., Yokota, K., and Fuchibe, K. (2004). *Angew. Chem. Int. Ed.* 43: 1566–1568.
14 Uraguchi, D. and Terada, M. (2004). *J. Am. Chem. Soc.* 126: 5356–5357.
15 Carroll, M.P. and Guiry, P.J. (2014). *Chem. Soc. Rev.* 43: 819–833.
16 Kočovský, P., Vyskočil, Š., and Smrčina, M. (2003). *Chem. Rev.* 103: 3213–3246.
17 Mikami, K., Aikawa, K., Yusa, Y. et al. (2002). *Synlett*: 1561.
18 Bringmann, G., Gulder, T., Gulder, T.A.M., and Breuning, M. (2011). *Chem. Rev.* 111: 563–639.
19 LaPlante, S.R., Fader, L.D., Fandrick, K.R. et al. (2011). *J. Med. Chem.* 54: 7005–7022.
20 Lanman, B.A., Allen, J.R., Allen, J.G. et al. (2020). *J. Med. Chem.* 63: 52–65.

21 Okamoto, Y. and Ikai, T. (2008). *Chem. Soc. Rev.* 37: 2593–2608.
22 Zhang, X., Yin, J., and Yoon, J. (2014). *Chem. Rev.* 114: 4918–4959.
23 Pu, L. (2017). *Acc. Chem. Res.* 50: 1032–1040.
24 Akagi, K. (2009). *Chem. Rev.* 109: 5354–5401.
25 Bisoyi, H.K. and Li, Q. (2014). *Acc. Chem. Res.* 47: 3184–3195.
26 Rivera-Fuentes, P. and Diederich, F. (2012). *Angew. Chem. Int. Ed.* 51: 2818–2828.
27 Wencel-Delord, J., Panossian, A., Leroux, F.R., and Colobert, F. (2015). *Chem. Soc. Rev.* 44: 3418–3430.
28 Bringmann, G. and Menche, D. (2001). *Acc. Chem. Res.* 34: 615–624.
29 Li, S., Zhang, J.-W., Li, X.-L. et al. (2016). *J. Am. Chem. Soc.* 138: 16561–16566.
30 Birman, V.B., Rheingold, A.L., and Lam, K.-C. (1999). *Tetrahedron: Asymmetry* 10: 125–131.
31 Zhang, J.-H., Liao, J., Cui, X. et al. (2002). *Tetrahedron: Asymmetry* 13: 1363–1366.
32 Bringmann, G., Price Mortimer, A.J., Keller, P.A. et al. (2005). *Angew. Chem. Int. Ed.* 44: 5384–5427.
33 Brussee, J. and Jansen, A.C.A. (1983). *Tetrahedron Lett.* 24: 3261–3262.
34 Prelog, V. and Helmchen, G. (1982). *Angew. Chem. Int. Ed.* 21: 567–583.
35 Prelog, V. and Helmchen, G. (1972). *Helv. Chim. Acta* 55: 2581–2598.
36 Cahn, R.S., Ingold, C., and Prelog, V. (1966). *Angew. Chem. Int. Ed.* 5: 385–415.
37 Cahn, R.S., Ingold, C.K., and Prelog, V. (1956). *Experientia* 12: 81–94.
38 Cahn, R.S. and Ingold, C.K. (1951). *J. Chem. Soc.*: 612–622.
39 Cahn, R.S. (1964). *J. Chem. Educ.* 41: 116.
40 Wang, C. and Wu, W. (2011). *J. Chem. Educ.* 88: 299–301.
41 Bhushan, R. and Bhattacharjee, G. (1983). *J. Chem. Educ.* 60: 191.